Int. J. Anal. Appl. (2025), 23:33

International Journal of Analysis and Applications

Energy Distribution Effect on Bremsstrahlung Radiation Produced by B_{11}^{5} and Al_{27}^{13}

R.J. Almatrafi*, S.A. Alkhateeb, N.A. Almuallem

Department of Mathematics and Statistics, Faculty of Science, University of Jeddah, Jeddah, Saudi Arabia

**Corresponding author:* ralmatrafi.stu@uj.edu.sa

Abstract. By using the Bethe-Heitler equation, this work determines the energy distribution of Bremsstrahlung radiation for B_{11}^{5} and Al_{27}^{13}. We utilize the mathematical program "Mathematica" to contrast the electromagnetic impacts of photons resulting from interactions of electrons with boron and aluminum nuclei. We compare the effects of electric and magnetic cross-sections on the generation of Bremsstrahlung radiation. We will examine the impact of electric and magnetic fields on the production of Bremsstrahlung radiation using graphs. We also investigate the effect of atom mass on the emission of Bremsstrahlung radiation. According to our results, certain types of X-rays can be produced by using magnetic interactions.

1. Introduction

In a variety of scientific applications, especially medical imaging, it is important to predict the energy and angle of the bremsstrahlung radiation generated by targets being bombarded with electrons ([1]). Advances in radiation physics, accelerator physics, and medical physics depend on an understanding of the distribution of photon emissions from an electron beam interacting with target materials. As an example, when a patient receives external radiation therapy, the shape and intensity of the beam are adjusted to improve the patient's dose distribution. How precisely doses are administered to the patient and how well quality assurance measures have been implemented to ensure that these doses stay accurate and have an impact on the results of radiation treatment ([2], [3], [4]).

Using gold and aluminum targets and an incident electron energy of 140 keV, Faulk and Quarles reported the first measurements of the energy distribution for fixed electron and photon directions in 1973 ([5]). The data were compared with the Elwert-Haug and with the Bethe-Heitler calculations, both theories generally agree with aluminum (Z = 13), and for gold (Z = 79) neither theory agrees satisfactorily with the data even though the Elwert-Haug theory is somewhat more accurate.

Received: Dec. 19, 2024.

2020 *Mathematics Subject Classification.* 81V10, 81T18, 78A70, 78A35.

Key words and phrases. Bremsstrahlung radiation; Bethe-Heitler equation; energy distribution; cross section.

https://doi.org/10.28924/2291-8639-23-2025-33
ISSN: 2291-8639

in-depth analysis of the energy dependence of the absolute cross section for gold was published in 1977 by Aehlig, Metzger, and Scheer ([6]), The incident electron energy was 300 keV. Over a broad range of photon energy, measurements were performed for four distinct combinations of electron scattering and emission angles. The deviations from the Bethe-Heitler formula were generally slightly larger than those from the Elwert-Haug calculations. For hard-photon emission (photon energies greater than 150 keV), the partial-wave computations of Keller and Dreizler ([7]) are in agreement with those presented by Shaffer et al ([8]). The partial-wave results of Keller and Dreizler and those of Tseng ([9]) agree fairly well with the experimental data in the hard-photon region for the angles $20°, -35°$, where the cross sections are much smaller. At lower photon energies less than 150 keV, however, there are significant differences between the theoretical curves. A set of parameters was used in Komma and Nakel's ([10]) measurements on gold targets, and the results of Elwert and Haug's and Bethe and Heitler's calculations show different behavior.

In the presence of atomic nuclei, they deflect or slow down charged particles, such as electrons, emitting electromagnetic radiation known as braking or bremsstrahlung radiation. Germany coined this term to quantify the electromagnetic radiation that charged particles emit. In the process of slowing down, electrons lose energy and produce radiation. Continuous radiation offers various applications, including medical imaging ([11], [12], [13]). When a charged particle approaches an atomic nucleus, like an electron, the nucleus' electric field influences it, exerting a force on the electron. As a result, the electron either breaks down or changes direction. The change in speed, known as braking radiation, generates electromagnetic radiation. The electron's speed and the field's force determine the energy of the released radiation, resulting in a spectrum of radiation with different wavelengths.

Electron-nuclei interactions, where the electron interacts with the nuclei field, produce bremsstrahlung photons ([14]). We can represent it as follows using the interaction equation:

$$e_i^- + N \rightarrow N + e_f^- + \gamma \tag{1.1}$$

Fig. 1 The Feynman diagrams for the bremsstrahlung radiation process are displayed.

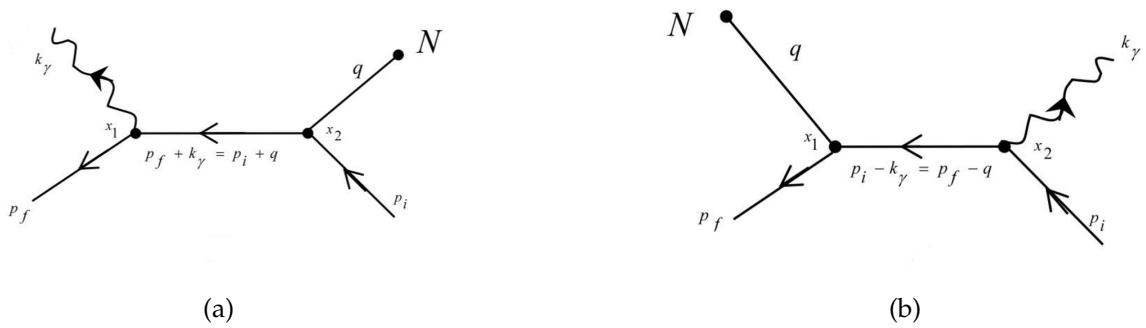

FIGURE 1. Feynman diagrams for bremsstrahlung processes

In a bremsstrahlung reaction, either (a) electrons interact with the atom's Coulomb field N, scatter, and then emit photons, or (b) the incident electron collides with the atom's Coulomb field, first emitting a photon before scattering electrons ([15], [16]).

In this paper, we aim to study the energy distribution of bremsstrahlung radiation of aluminum $(Z = 13)$ and boron $(Z = 5)$ atoms with incident angles of $80°, 100°, 120°$. There is an energy range of 300 GeV to 1000 GeV for the incident electrons.

2. Methodology

Electrons with energy ranging from 300 GeV to 1000 GeV collided with a boron atom with atom number 5 and an aluminum atom with atom number 13 ([17]), leading to the production of bremsstrahlung. This process can be illustrated in Figure 2.

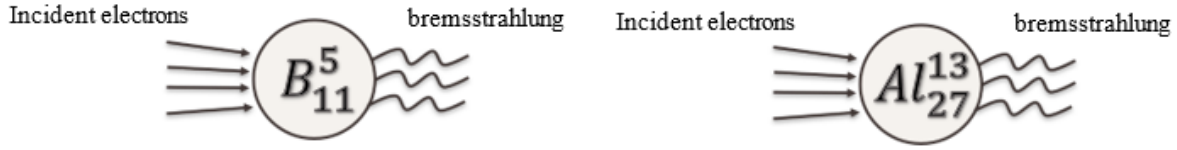

Figure 2. Bremsstrahlung Radiation Emitted by Incident Electrons on B_{11}^{5} and Al_{27}^{13} Targets.

The radiation equation ([15], [18], [19]) describes the Bremsstrahlung radiation cross-sections, predicting the rate at which photons are emitted when electrons are decelerated in the Coulomb field of an atomic nucleus and can be written as ([20], [21]):

$$d\sigma = \mathrm{d}\sigma_{\mathrm{EC}} + \mathrm{d}\sigma_{\mathrm{MD}} + \mathrm{d}\sigma_{\mathrm{EQ}} + \mathrm{d}\sigma_{\mathrm{MO}} \tag{2.1}$$

It is important to understand that the symbols $\mathrm{d}\sigma_{\mathrm{EC}}, \mathrm{d}\sigma_{\mathrm{MD}}, \mathrm{d}\sigma_{\mathrm{EQ}}$, and $\mathrm{d}\sigma_{\mathrm{MO}}$ are, respectively, electric charge (EC), magnetic dipole (MD), electric quadrupole (EQ), and magnetic octupole (MO). Such that $\mathrm{d}\sigma_{\mathrm{EC}}$ and $\mathrm{d}\sigma_{\mathrm{EQ}}$ represent the electric cross sections, while $d\sigma_{MD}$ and $d\sigma_{MO}$ represent the magnetic cross sections.

The following equations can represent these electrical and magnetic cross-sections ([22]):

$$\mathrm{d}\sigma_{EC} = 8\pi\zeta\phi_{EC}, \tag{2.2}$$

$$\mathrm{d}\sigma_{\mathrm{MD}} = 8\pi\zeta\left(\frac{\mu_1}{\mathrm{z}\times e}\right)^2 a_{MD}\phi_{MD}, \tag{2.3}$$

$$\mathrm{d}\sigma_{\mathrm{EQ}} = 8\pi\zeta\left(\frac{Q}{\mathrm{zxe}}\right)^2 a_{EQ}\phi_{EQ}, \tag{2.4}$$

$$\mathrm{d}\sigma_{\mathrm{MO}} = 8\pi\zeta\left(\frac{\Omega}{\mathrm{zxe}}\right)^2 a_{MO}\phi_{MO}, \tag{2.5}$$

Such that,

$$\zeta = \frac{z_1^2\alpha^3}{4\pi^2}\frac{k_+}{k_-\times\chi}, \tag{2.6}$$

$$a_{MD} = \frac{s+1}{3s}, \tag{2.7}$$

$$a_{EQ} = \frac{(s+1)((2s)+3)}{180s((2s)-1)}, \tag{2.8}$$

$$a_{MO} = \frac{2(s+1)(s+2)((2s)+3)}{4725s(s-1)((2s)-1)}. \tag{2.9}$$

Are the a_{MD}, a_{EQ} and a_{MO} coefficients of the nucleus with spin s. (where s = 1.5 for boron atom and equals 2.5 for aluminum atom) ([23]).

The functions of electric fields (charge and quadrupole) and magnetic fields (dipole and octupole) can be represented by the equations ([19], [20], [21], [24]):

$$\begin{aligned}\phi_{EC} &= \frac{2\gamma-7}{8{k_0}^2\omega^2\Delta^2} - \frac{1-\gamma^2}{8\beta^2\Delta^2} + \frac{1-\gamma}{4{k_0}^2\omega^2\Delta} - \frac{\epsilon_0}{4{k_0}^2\omega^2\Delta(1-\gamma)} \\ &- \left(\frac{\epsilon_t}{8{k_0}^2\omega^2\beta\Delta(1-\gamma)}\left(3\gamma + \frac{{k_0}^2\omega^2}{\beta^2}\gamma(1-\gamma)^2\right)\right) \\ &+ \left(\frac{L}{8{k_0}^2\omega^2\Delta^2(1-\gamma)}\left(2+2(1-\gamma)^2+\gamma(2-\gamma)\Delta\right)\right),\end{aligned} \tag{2.10}$$

$$\begin{aligned}\phi_{MD} &= \frac{-3}{2} + \frac{{k_0}^2\omega^2}{2\beta^2\Delta}\gamma(1-\gamma-\Delta) + \frac{\epsilon_0}{2(1-\gamma)}\left(1-\gamma+\frac{1+(1-\gamma)^2}{\Delta}\right) + \frac{\epsilon_t}{2\beta^3}{k_0}^2\omega^2\frac{\gamma^2(1-\gamma+\gamma\Delta)}{(1-\gamma)} \\ &+ \frac{L}{4(1-\gamma)},\end{aligned} \tag{2.11}$$

$$\begin{aligned}\phi_{EQ} &= {k_0}^2\omega^2(4-\gamma)\Delta - 2{k_0}^2\omega^2\left(1+(1-\gamma)^2\right) + \frac{{k_0}^2\omega^2}{\Delta}(1-\gamma)\left(1+(1-\gamma)^2\right) \\ &+ \frac{\epsilon_0}{2(1-\gamma)}{k_0}^2\omega^2\left(1+(1-\gamma)^2\right)(2 \\ &- \Delta\ ),\end{aligned} \tag{2.12}$$

$$\begin{aligned}\phi_{MO} &= {k_0}^4\omega^4\left(\frac{20}{3\Delta}(1-\gamma)^3\left(1+(1-\gamma)^2\right) - 12(1-\gamma)^4 + 2(1-\gamma)\left(5+2\gamma+7(1-\gamma)^2\right)\right. \\ &- 4\Delta\left(2-\gamma^2+\gamma^3\right) - \frac{4}{3}\left(6+(1-\gamma)^2\right)\Delta \\ &\left.+ \frac{\epsilon_0}{1-\gamma}\left(1+(1-\gamma)^2\right)\Delta(2+\Delta)\right),\end{aligned} \tag{2.13}$$

Where,

$$\gamma = 0.5, E_- = \frac{\epsilon}{\gamma}, E_+ = E_- - \epsilon, \chi = \frac{\epsilon}{ch}, \omega = \frac{E_-}{0.511}, \tag{2.14}$$

$$\Delta = 1 - \mathrm{Cos}[\theta] \tag{2.15}$$

$$k_0 = \frac{m_0 c}{h}, T_0 = \sqrt{(1-\gamma)^2 + (2\gamma\Delta)}, \beta = k_0\omega T_0, \tag{2.16}$$

$$L = 2\log\left[\frac{2\omega(1-\gamma)}{\gamma}\right], \epsilon_0 = 2\log[2\omega(1-\gamma)], \epsilon_t = \log\left[\frac{\beta-\gamma+1}{\beta+\gamma+1}\right]. \tag{2.17}$$

3. Results

In this section, we Calculations were performed using the Mathematica program, which was utilized to implement the Bethe-Heitler equation, separate the differential cross-section into electric and magnetic cross-sections, and generate graphs of cross-sections across energy distributions ranging from 300 to 1000 GeV at incident angles of $80°, 100°$, and $120°$. Based on these analyses, we conclude the following:

3.1. Effect of electric and magnetic cross sections on the boron atom.

- The electrical cross sections of boron nuclei decrease with increasing energy and angle of incidence. as shown in Figure 3. for example:

$$d\sigma_{E1} = 1.6025 \times 10^{-34} \quad \text{at } \epsilon = 500\,\text{GeV and } \theta = 80°$$
$$d\sigma_{E1} = 5.94454 \times 10^{-35} \quad \text{at } \epsilon = 500\,\text{GeV and } \theta = 100°$$

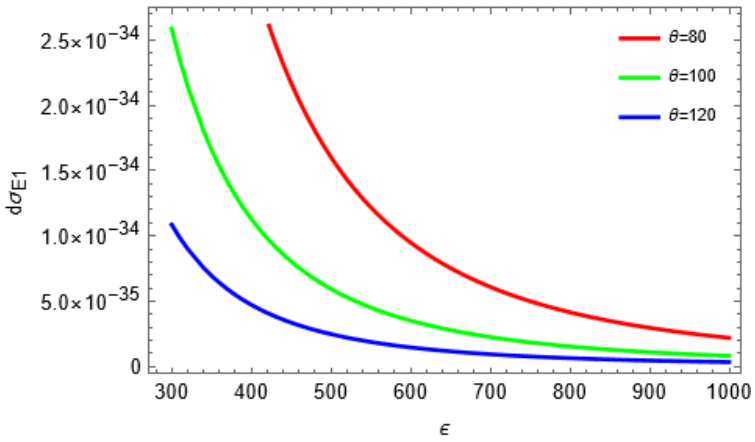

Figure 3. Electric cross-sections for B_{11}^{5} atom at $\theta = 80°, 100°, 120°$. Note that $d\sigma_{E1}$ is more effective at energy $\epsilon = 300$GeV and angle $\theta = 80°$.

- The magnetic cross-sections of boron nuclei increase as both the energy and incident angle increase. as shown in Figure 4. for example:

$$d\sigma_{M1} = 5.0969 \times 10^{-20} \quad \text{at } \epsilon = 800\,\text{GeV and } \theta = 100°$$
$$d\sigma_{M1} = 7.14813 \times 10^{-20} \quad \text{at } \epsilon = 800\,\text{GeV and } \theta = 120°$$

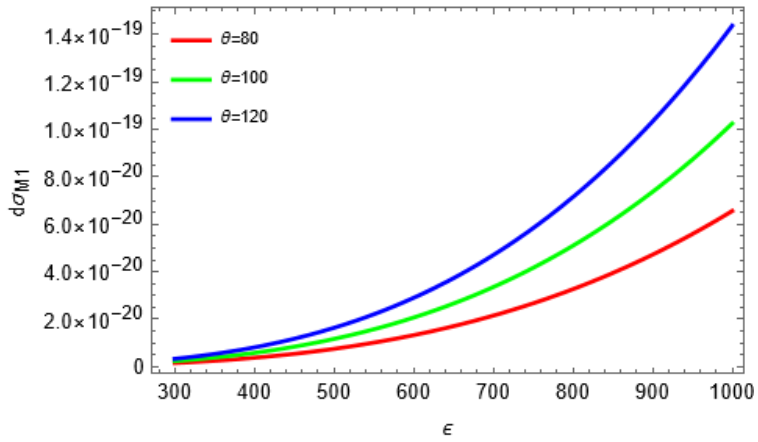

FIGURE 4. Magnetic cross-sections for B_{11}^{5} atom at $\theta = 80°, 100°, 120°$. Note that $d\sigma_{M1}$ is more effective at energy $\epsilon = 1000$GeV and angle $\theta = 120°$.

3.2. Effect of electric and magnetic cross sections on the aluminum atom.

- The electric cross-sections of aluminum nuclei decrease as the energy and incident angle increase.as shown in Figure 5. for example:

$$d\sigma_{E2} = 6.41969 \times 10^{-34} \quad \text{at } \epsilon = 600\,\text{GeV and } \theta = 80°$$

$$d\sigma_{E2} = 9.93894 \times 10^{-35} \quad \text{at } \epsilon = 600\,\text{GeV and } \theta = 100°$$

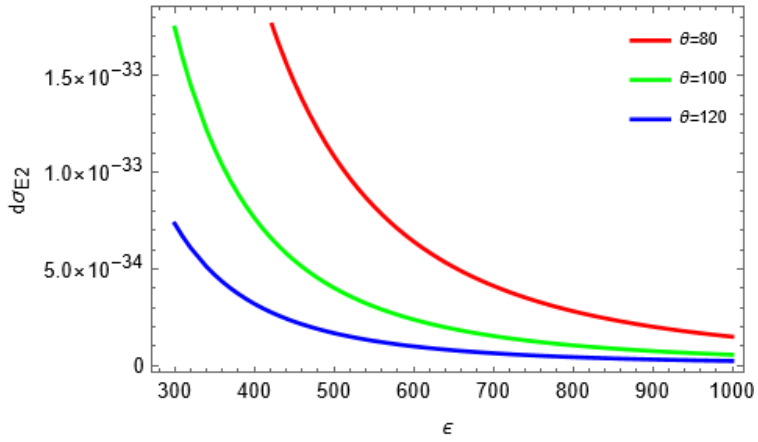

FIGURE 5. Electric cross-sections for Al_{27}^{13} atom at $\theta = 80°, 100°, 120°$. Note that $d\sigma_{E2}$ is more effective at energy $\epsilon = 300$Gev and angle $\theta = 80°$.

- The magnetic cross-sections of aluminum nuclei increase as the energy and incident angle increase .as shown in Figure 6.For example:

$$d\sigma_{M2} = 1.51693 \times 10^{-20} \quad \text{at } \epsilon = 1000\,\text{GeV and } \theta = 100°$$

$$d\sigma_{M2} = 2.12773 \times 10^{-20} \quad \text{at } \epsilon = 1000\,\text{GeV and } \theta = 120°$$

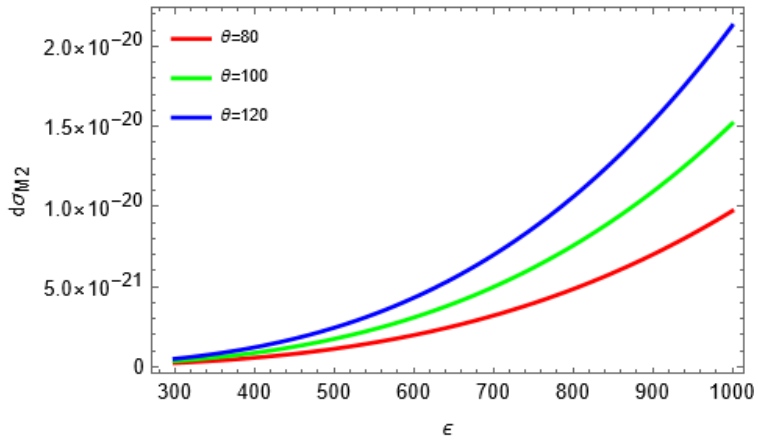

FIGURE 6. Magnetic cross-sections for Al_{27}^{13} atom at $\theta = 80°, 100°, 120°$. Note that $d\sigma_{M2}$ is more effective at energy $\epsilon = 1000$Gev and angle $\theta = 120°$.

3.3. Effect of atomic number.

- The electrical cross-sectionss of the aluminum atom are more effective in producing Bremsstrahlung radiation than the electrical cross sections of the boron atom, as shown in Figure 7.For example:

$$d\sigma_{E1} = 3.44902 \times 10^{-36} \quad \text{at } \epsilon = 1000$$
$$d\sigma_{E2} = 2.36732 \times 10^{-35} \quad \text{at } \epsilon = 1000$$

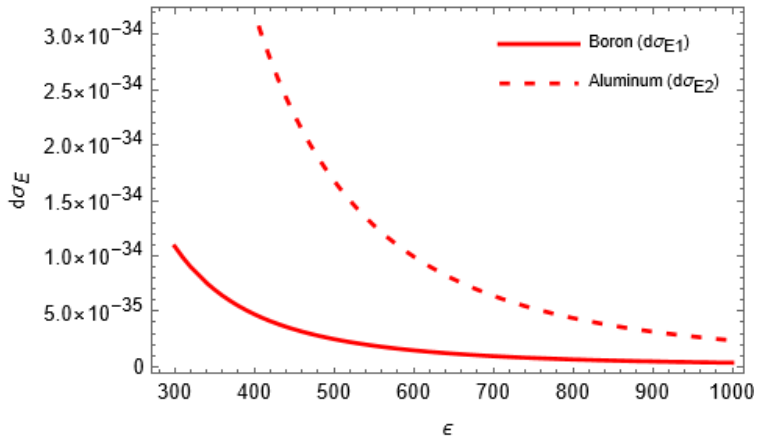

FIGURE 7. Comparison of electric cross-sections of B_{11}^{5}, Al_{27}^{13} at $\theta = 120°$. Note that the electric cross-sections of the higher-mass aluminum ($Z = 27$) are more effective in producing Bremsstrahlung radiation than those of the lighter-mass boron ($Z = 11$).

- The magnetic cross-sections of the boron atom are more effective in producing Bremsstrahlung radiation than the magnetic cross-sections for the aluminum atom. as shown in Figure 8. for example:

$$d\sigma_{M1} = 2.14898 \times 10^{-20} \quad \text{at } \epsilon = 700$$

$$d\sigma_{M2} = 3.17971 \times 10^{-21} \quad \text{at } \epsilon = 700$$

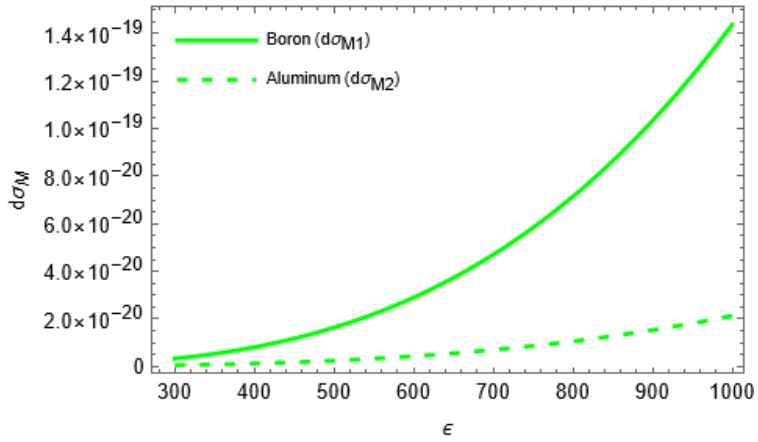

FIGURE 8. Comparison of magnetic cross-sections of B_{11}^{5}, Al_{27}^{13} at $\theta = 120°$. Note that the magnetic cross-sections of lighter mass boron ($Z = 11$) are more effective in producing Bremsstrahlung radiation than those of the higher mass aluminum ($Z = 27$).

4. CONCLUSION

Bremsstrahlung radiation, generated when atomic nuclei decelerate high-energy electrons, is significant in various fields, from medical imaging to nuclear physics. The Bethe-Heitler equation is a mathematical model for figuring out the bremsstrahlung cross-section. It predicts how the differential cross-section will change with energy and atomic number. This study focuses on B_{11}^{5} and Al_{27}^{13}. The study takes into account the energy distribution of boron and aluminum atoms in the $300 - 1000$ GeV energy range, as well as the incident angles $80°, 100°, 120°$. This study contributes to understanding Bremsstrahlung radiation. We found that the magnetic cross sections of two nuclei, boron and aluminum, are more effective than the electrical cross sections at producing Bremsstrahlung radiation. By looking at boron and aluminum as nuclei side by side, we discovered that the higher-mass aluminum ($Z = 27$) has better electrical cross sections for making Bremsstrahlung radiation than the lower-mass boron ($Z = 11$), and the lowermass boron ($Z = 11$) has better magnetic cross sections for making Bremsstrahlung radiation than the higher-mass aluminum ($Z = 27$). This study provides support for recent studies ([25], [26], [27]) that assert the importance of magnetic interactions in Bremsstrahlung processes.

Conflicts of Interest: The authors declare that there are no conflicts of interest regarding the publication of this paper.

References

[1] A. Omar, P. Andreo, G. Poludniowski, Performance of Different Theories for the Angular Distribution of Bremsstrahlung Produced by keV Electrons Incident upon a Target, Radiat. Phys. Chem. 148 (2018), 73–85. https://doi.org/10.1016/j.radphyschem.2018.02.009.

[2] I.J. Das, C. Cheng, R.J. Watts, A. Ahnesjö, J. Gibbons, X.A. Li, J. Lowenstein, R.K. Mitra, W.E. Simon, T.C. Zhu, Accelerator Beam Data Commissioning Equipment and Procedures: Report of the TG-106 of the Therapy Physics Committee of the AAPM, Med. Phys. 35 (2008), 4186–4215. https://doi.org/10.1118/1.2969070.

[3] G.J. Kutcher, L. Coia, M. Gillin, et al. Comprehensive QA for Radiation Oncology: Report of AAPM Radiation Therapy Committee Task Group 40, Med. Phys. 21 (1994), 581–618. https://doi.org/10.1118/1.597316.

[4] E.E. Klein, J. Hanley, J. Bayouth, et al. Task Group 142 Report: Quality Assurance of Medical Acceleratorsa), Med. Phys. 36 (2009), 4197–4212. https://doi.org/10.1118/1.3190392.

[5] J.D. Faulk, C.A. Quarles, Coincidence Measurement of the Fully Differential Cross Section for Atomic-Field Bremsstrahlung, Phys. Rev. A 9 (1974), 732–742. https://doi.org/10.1103/PhysRevA.9.732.

[6] A. Aehlig, L. Metzger, M. Scheer, Measurement of the Absolute Cross Section for the Elementary Process of Atomic Field Bremsstrahlung, Z. Phys. A 281 (1977), 205–209. https://doi.org/10.1007/BF01408838.

[7] C.D. Shaffer, X.-M. Tong, R.H. Pratt, Triply Differential Cross Section and Polarization Correlations in Electron Bremsstrahlung Emission, Phys. Rev. A 53 (1996), 4158–4163. https://doi.org/10.1103/PhysRevA.53.4158.

[8] S. Keller, R.M. Dreizler, Relativistic Independent Particle Approximation Study of Triply Differential Cross Sections for Electron - Atom Bremsstrahlung, J. Phys. B 30 (1997), 3257–3266. https://doi.org/10.1088/0953-4075/30/14/016.

[9] H.K. Tseng, Relativistic Calculation of the Unpolarized Triple-Differential Cross Section and the Polarization Correlation of the Electron Bremsstrahlung from Atoms, J. Phys. B 35 (2002), 1129–1142. https://doi.org/10.1088/0953-4075/35/5/301.

[10] M. Komma, W. Nakel, Two-Parameter Coincidence Measurements of Bremsstrahlung, Electron-Electron Bremsstrahlung, and K-Shell Ionisation for 300 keV Electron Impact, J. Phys. B 15 (1982), 1433–1441. https://doi.org/10.1088/0022-3700/15/9/018.

[11] E. Haug, W. Nakel, The Elementary Process of Bremsstrahlung, World Scientific, Singapore, 2004.

[12] J.D. Jackson, Classical Electrodynamics, John Wiley & Sons, New York, 2021.

[13] D. Greenberger, K. Hentschel, F. Weinert, eds., Compendium of Quantum Physics: Concepts, Experiments, History and Philosophy, Springer, Berlin, Heidelberg, 2009. https://doi.org/10.1007/978-3-540-70626-7.

[14] S. Al-Khateeb, Polarization Dependence of the Bremsstrahlung Cross-Section in the Scattering of Electrons by Nuclei with Electromagnetic Multipole Moments, J. King Abdulaziz Univ.-Sci. 23 (2011), 65–78. https://doi.org/10.4197/Sci.23-2.5.

[15] S.H. Morgan, Coulomb Corrections to the Bethe-Heitler Cross Sections for Electron-Nucleus Bremsstrahlung, NASA Technical Reports Server, (1970). https://ntrs.nasa.gov/citations/19710001524.

[16] R.P. Feynman, Quantum Electrodynamics, CRC Press, Boca Raton, 2018.

[17] A. Beiser, Concepts of Modern Physics, McGraw-Hill, New York, 2003.

[18] W. Zhu, Improved Bethe-Heitler Formula, Nucl. Phys. B 953 (2020), 114958. https://doi.org/10.1016/j.nuclphysb.2020.114958.

[19] W. Greiner, J. Reinhardt, Quantum Electrodynamics, Springer, Berlin, 2008.

[20] S.A. Alkhateeb, A.A. Alshaery, and R.A. Aldosary, Electron-positron pair production in electromagnetic field, J. Appl. Math. Phys. 10 (2022), 237–244. https://doi.org/10.4236/jamp.2022.102017.

[21] S.A. Alkhateeb, A.A. Alshaery, and R.A. Aldosary, Leptonic Pair Production in Electro Magnetic Field, Nucl. Sci. 7 (2022), 34–38.

[22] S. Alkhateeb, Effect of Nuclear Magnetic Distribution on Thephoto Production of Longitudinally Polarizedlepton-Pairs in the Field of Na2311 and Al2713 Nuclei, Therm. Sci. 24 (2020), 139–147. https://doi.org/10.2298/TSCI20S1139A.

[23] N.J. Stone, Table of Nuclear Magnetic Dipole and Electric Quadrupole Moments, At. Data Nucl. Data Tables 90 (2005), 75–176. https://doi.org/10.1016/j.adt.2005.04.001.

[24] H. Bethe, W. Heitler, On the Stopping of Fast Particles and on the Creation of Positive Electrons, Proc. R. Soc. Lond. A. 146 (1934), 83–112. https://doi.org/10.1098/rspa.1934.0140.

[25] M. Habibi, A. Arefiev, T. Toncian, High Field Suppression of Bremsstrahlung Emission in High-Intensity Laser–Plasma Interactions, Phys. Plasmas 30 (2023), 103108. https://doi.org/10.1063/5.0167288.

[26] P. Fischer, Frontiers in Imaging Magnetism with Polarized X-Rays, Front. Phys. 2 (2015), 82. https://doi.org/10.3389/fphy.2014.00082.

[27] C.-T. Liao, C. Hernández-García, M.M. Murnane, Switching the Twist in X Rays with Magnets, Physics 14 (2021), 34. https://doi.org/10.1103/Physics.14.34.